Journal of Power Sources 296 (2015) 290–297

Contents lists available at ScienceDirect

Journal of Power Sources

journal homepage: www.elsevier.com/locate/jpowsour

Enhanced formic acid oxidation on polycrystalline platinum modified by spontaneous deposition of gold. Fourier transform infrared spectroscopy studies

Paula S. Cappellari [a], Gonzalo García [b], Jonathan Florez-Montaño [b], Cesar A. Barbero [a], Elena Pastor [b], Gabriel A. Planes [a, *]

[a] Universidad Nacional de Río Cuarto. RutaNac. 36, Km 601, Río Cuarto, Córdoba, Argentina
[b] Instituto Universitario de Materiales y Nanotecnología, Universidad de La Laguna, Av. Astrofísico F. Sánchez s/n, 38071 La Laguna, Tenerife, Spain

HIGHLIGHTS

- The Pt surface was modified by spontaneous (electroless) deposition of gold atoms.
- Two reaction pathways are clearly identified for HCOOH electro-oxidation on Pt and PtAu.
- HCOOH oxidation on Pt surfaces prefers the indirect route (dehydration).
- The direct pathway (dehydrogenation) for HCOOH oxidation is favored at PtAu electrodes.
- The performance toward the HCOOH oxidation is greatly enhanced by PtAu electrodes.

GRAPHICAL ABSTRACT

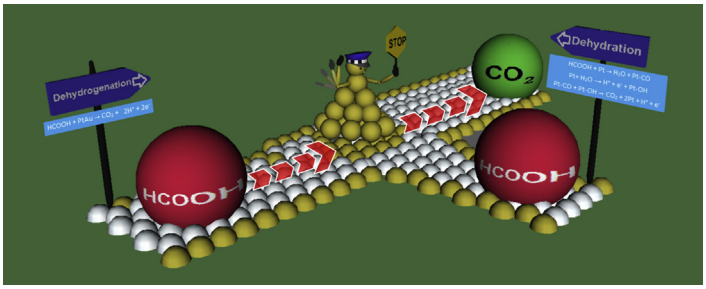

ARTICLE INFO

Article history:
Received 11 February 2015
Received in revised form
15 May 2015
Accepted 3 July 2015
Available online xxx

Keywords:
Formic acid
PtAu
Electroless
In-situ FTIR

ABSTRACT

Formic acid and adsorbed carbon monoxide electrooxidation on polycrystalline Pt and Au-modified Pt surfaces were studied by cyclic voltammetry, lineal sweep voltammetry and *in-situ* Fourier transform infrared spectroscopy techniques. With this purpose, a polycrystalline Pt electrode was modified by spontaneous deposition of gold atoms, achieving a gold surface coverage (θ) in the range of $0 \leq \theta \leq 0.47$. Results indicate the existence of two main pathways during the formic acid oxidation reaction, i.e. dehydration and dehydrogenation routes. At higher potentials than 0.5 V the dehydrogenation pathway appears to be the operative at both Pt and Au electrodes. Meanwhile, the dehydration reaction is the main pathway for Pt at lower potentials than 0.5 V. It was found that reaction routes are easily tuned by Au deposition on the Pt sites responsible for the formic acid dehydration reaction, and hence for the catalytic formation of adsorbed carbon monoxide. Gold deposition on these Pt open sites produces an enhanced activity toward the HCOOH oxidation reaction. In general terms, the surface inhibition of the reaction by adsorbed intermediates (indirect pathway) is almost absent at gold-modified Pt electrodes, and therefore the direct pathway appears as the main route during the formic acid electrooxidation reaction.

* Corresponding author.
E-mail addresses: pcappellari@exa.unrc.edu.ar (P.S. Cappellari), ggarcia@ull.es (G. García), jnaz16@gmail.com (J. Florez-Montaño), cbarbero@exa.unrc.edu.ar (C.A. Barbero), epastor@ull.edu.es (E. Pastor), gplanes@exa.unrc.edu.ar (G.A. Planes).

http://dx.doi.org/10.1016/j.jpowsour.2015.07.005
0378-7753/

1. Introduction

The use of liquid fuel in low temperature polymeric electrolyte membrane fuel cells (PEMFC) combines the advantage of high power density and the simplicity of fuel handling. Comparing with methanol, the use of formic acid as fuel allows a higher open circuit potential, a reduced fuel crossover and a higher practical energy conversion efficiency [1,2].

Recently, PtAu materials were used as catalysts for formic acid electrooxidation (FAEO) [3–6]. Main result indicates an enhancement of the faradaic current during the formic acid oxidation on PtAu in comparison with Pt electrodes. The last is not completely understood, although the surface composition and the surface structure of the electrodes appear as the main responsible for the FAEO enhancement. On the other hand, it is well-known the poisoning effect of adsorbed reaction intermediates (e.g. CO) on Pt surface during the FAEO. However, the role of Au atoms in the PtAu electrode and their incidence on the formation and/or elimination of such chemical species is controversial [7].

It is currently assumed that Au atoms block some key sites for CO adsorption, avoiding in this way the Pt surface deactivation by poisoning species and the consequent activation of other site-demanding FAEO pathways (e.g. dehydrogenation) [8]. Considering the irreversible nature of the Pt surface modification by Au atoms, the surface site blocking effect may produce a time-stable influence over the HCOOH electrooxidation, i.e. site knockout effect [9].

Recently, it has been proposed that well dispersed Au atoms on Pt decomposes HCOOH at near ambient temperatures (350 K) to form mainly H_2 and CO_2 [10]. It was suggested that Au atoms facilitate the first electron transfer during the HCOOH electrooxidation to $HCOO_{ads}$ and assist the effective spillover of adsorbed formate from Au to Pt sites, where it is further oxidized to CO_2 [6]. In this context, *in situ* surface-enhanced Raman spectroscopy (SERS) revealed the participation of formate as the main intermediate during the electrooxidation process of HCOOH on Pt modified Au surface [11].

The aim of the present work is to establish the role of Au atoms during the electrooxidation of formic acid on a polycrystalline Pt (Pt_{pc}) electrode modified by spontaneous (electroless) gold deposition (Au coverage $0 \leq \theta \leq 0.47$). With this purpose, the adsorption and oxidation of CO by direct exposition to dissolved CO or formed during the HCOOH oxidation was followed applying *in-situ* Fourier transform infrared spectroscopy (FTIRS), lineal sweep voltammetry (LSV) and cyclic voltammetry (CV). Finally, the results were discussed in terms of surface structure and surface composition.

2. Experimental

2.1. Materials

Sulphuric acid (98% w/w), formic acid (85% w/w) and perchloric acid (70% w/w) were purchased from Cicarelli. Gold tetrachloroauric acid (trihydrate; 99.5%) was purchased from Sigma–Aldrich. All reactants were used as received. Solutions were prepared from ultra-pure water (18.2 MΩ cm, from Milli-Q Water Purification System).

2.2. Preparation of Au-modified platinum electrode surface by spontaneous deposition

A polycrystalline platinum rod (3 mm diameter) embedded in a Teflon holder was used as substrate. The exposed Pt disk was polished with diamond paste (3, 1 and 0.5 μm), sonicated in acetone and ultra-pure water. For Au-modified platinum electrode, the Pt electrode was soaked in a 1 mM $AuHCl_4$/0.5 M $HClO_4$ solution during 15 min and after that, it was raised and washed copiously with ultra-pure water. The electrode is then cycled between 0.05 and 1.5 V_{RHE} until a reproducible and stable cyclic voltammogram (CV) response was obtained at 50 mV/s. The percentage of Au coverage is calculated by the diminution of the charge in the Pt hydrogen adsorption/desorption region, assuming 210 μCcm^{-2} for a monolayer of adsorbed hydrogen. Typically, a gold coverage of 20–30 % is achieved for the first exposition to $HAuCl_4$ solution. Higher Au coverage can be obtained by successive $HAuCl_4$ expositions.

The process described above for electrode modification is highly reproducible (in terms of coverage, close to 2% of discrepancy between experiments). However, is necessary to assuring some key points. First, the protocol for electrode cleaning; and second, the use of aged Au solution should be avoided. On the other hand, the use of different Au concentrations may modify the time necessary to reach a given coverage. However, the electrochemical response is only dependent on the Au coverage.

2.3. Electrochemical experiments

An electrochemical cell with a three-electrode configuration was used for all electrochemical experiments. The cell was designed to allow solution exchange holding the potential control of the working electrode (WE). The WE was a polycrystalline platinum rod (3 mm dia.) embedded in a Teflon holder used with or without further Au modification, as described above. A reversible hydrogen electrode (RHE) and a platinum wire were used as reference and counter electrodes, respectively. All potentials in this work are given against the RHE. All measurements were implemented in deoxygenated solutions under argon atmosphere with an Autolab (Eco-chemie) potentiostat-galvanostat. The experiments were conducted at 25 °C.

CO stripping experiments were performed after bubbling CO through the cell for 5 min while keeping the WE electrode at 0.07 V, followed by argon purging for 15 min and electrolyte exchange to remove the excess of CO. CO stripping voltammograms were recorded by scanning the potential positively up to 0.90 V.

To study the effect of different exposition times of formic acid, the WE was immersed in 0.1 M HCOOH/0.5 M H_2SO_4 or 0.1 M HCOOH/0.5 M $HClO_4$ solution under potential control (0.25 V) for a specific time ($1 \leq t \leq 600$ s) and subsequently the lineal sweep voltammogram (LSV) was recorded by scanning positively up to 1.1 V.

The adsorbate coverage from the HCOOH dehydration reaction as function of the applied/adsorption potential (E_{ad}), was determined in a 0.1 M HCOOH/0.5 M H_2SO_4 solution at 25 °C. With this purpose, the WE was immersed in the formic acid solution at fix potential ($0.1 \leq E_{ad} \leq 0.6$ V) during 300 s, afterward the HCOOH was eliminated by electrolyte exchange (under potential control), and finally the potential was scanned positively.

2.4. In-situ FTIRS experiments

In-situ Fourier transform infrared spectra (FTIRS) were collected with a Bruker Vector 22 spectrometer equipped with a homemade spectroelectrochemical glass cell with a 60° CaF_2 prism at the bottom. It was designed for external reflection mode in a thin layer configuration. FTIR spectra were collected from an average of 128 scans and resolution of 8 cm^{-1}. Experience consists in the introduction of the WE in the formic acid solution (0.5 M HCOOH + 0.5 M $HClO_4$) at fix potential of 0.6 V. After 10 min of setup stabilization, the potential was stepped to the reference potential ($R_0 = 0.05$ V) and then single potential steps of 0.05 V in the

positive-going direction up to 1.0 V were performed. Spectra are represented as the ratio R/R_0, where R and R_0 are the reflectance measured at the sample and the reference potential, respectively. Consequently, positive and negative bands correspond to the loss and gain of species at the sample potential, respectively [12]. In order to avoid anion adsorption FTIRS experiments were carried out in perchloric acid.

3. Results and discussion

Fig. 1 shows the cyclic voltammograms for Pt_{pc} and Pt_{pc} modified with Au ($\theta = 34$ and 47%) in the base electrolyte. The hydrogen adsorption/desorption region (E < 0.4 V) of the unmodified electrode shows the typical features of Pt_{pc}, in which the currents associated to sites with (111), (110) and (100) orientations can be discerne0d [13–15]. Additionally to these features, Pt oxidation presents an onset potential at ca. 0.8 V, while its reduction develops a cathodic peak centered at ca. 0.75 V. The Au modification produces an increment of the anodic current at E > 1.3 V and the development of a peak around 1.15 V during the negative going scan. These faradaic currents are associated to the surface gold oxide formation and its reduction, respectively. Also, a clear diminution of the anodic charge associated to Pt oxidation (and consequently its reduction) can be discerned after gold deposition. The last can be the result of Pt blocking sites by gold atoms. In fact, after Pt modification with Au, the peak at 0.11 and 0.24 V, associated with hydrogen adsorption/desorption at Pt sites with (110) and (100) orientations, are clearly suppressed. Therefore, gold atom blocks mainly Pt sites with (110) and (100) orientations.

Fig. 2 shows the CO stripping curves for Pt_{pc} and Au-modified Pt_{pc} (coverage θ = 34 and 47%). The Pt electroactive areas obtained from the CO stripping experiments (0.147 cm^2 for $\theta = 34$ and 0.122 cm^2 for θ = 47%, assuming that the oxidation charge for a monolayer adsorption of CO on the Pt surface is 420 μCcm^{-2}) are similar to those obtained from H_{ad} (0.140 cm^2 for θ = 34 and 0.113 cm^2 for θ = 47%, assuming that the reduction charge for a monolayer adsorption of H on the Pt surface is 210 μCcm^{-2}). This small difference is also present for the unmodified Pt_{pc} (0.215 cm^2 for H_{ad} and 0.221 cm^2 for CO), and can be ascribed to uncertainty in the baseline correction of the CO stripping. Carbon monoxide and hydrogen only adsorb on platinum in the present conditions, and therefore gold simply blocks H and CO adsorption. In other words, the first effect of gold deposition is the decrease of the Pt active surface area.

Fig. 2 shows that the CO stripping peak shifts toward more positive potentials with the addition of gold onto the catalyst surface and this shift is proportional to the Au surface coverage. The later indicates that the oxidation of adsorbed CO is inhibited with the gold insertion and therefore the catalyst becomes less tolerant to CO. CO oxidation reaction requires of contiguous adsorbed oxygenated species at the surface (OH_{ad}), or at least considerable CO surface mobility to reach such sites [16]. Accordingly, the presence of Au may block the CO surface diffusion and especially it appears to inhibit the OH_{ad} formation, i.e. the water oxidation reaction. In this context, it is well-known that Pt open surfaces, such as (110), (100), and defect sites, are more reactive than a compact surface (e.g. Pt(111)), toward the water dissociation reaction [17]. In consequence, the shift of the oxidation peak towards more positive potentials and the absence of the oxidation current at ca. 0.5 V can be related with the decrease of Pt open surface structures after Au deposition onto Pt. Finally, it is reasonable to think that Au deposits specifically on open rather than compact surfaces, which is in total agreement with the observed behavior at the hydrogen adsorption/desorption region (Fig. 1). Consequently, the hydrogen adsorption/desorption region in the blank voltammogram (Fig. 1) and the CO stripping (Fig. 2) of Pt_{pc} modified with Au resembles that of Pt nanoparticles with short mean length of the (111) domains.

The catalytic activity of Au modified electrodes toward formic acid electrooxidation was studied by LSV (Fig. 3A) and compared to those obtained at Pt_{pc}. To understand the effect of formic acid exposition at controlled WE potential, the WE was immersed in 0.1 M HCOOH/0.5 M H_2SO_4 or 0.1 M HCOOH/0.5 M $HClO_4$solutions under potential control (0.25 V) during a specific time t_c($1 < t_c < 600$ s) previous to the forward scan (denoted as exposition time = t_c). Note that for short exposition times ($t_c < 10$ s), the voltammogram looks like to those described in the literature [18], developing two anodic peaks: (I) a broad peak centered at 0.4–0.6 V, and (II) a narrow peak located at 0.8–1.0 V. Furthermore, the faradaic charge involved in both anodic peaks increases from t_c 1–10 s. However, the anodic charge involved under the peak I

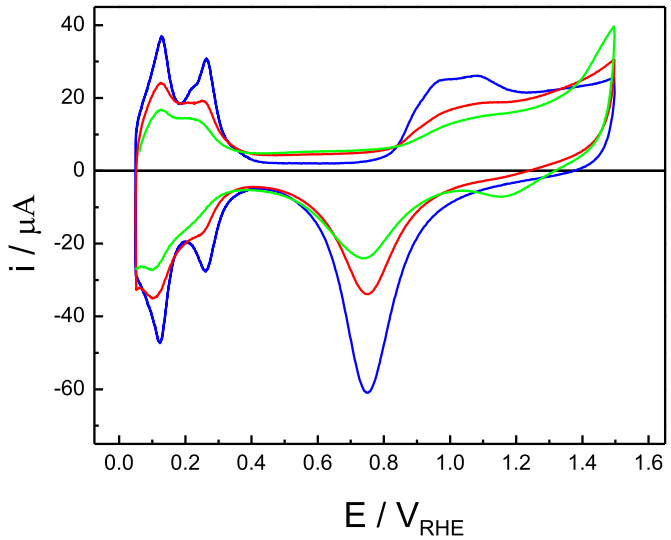

Fig. 1. Cyclic voltammogram for Pt (blue line) and PtAu electrodes with Au coverage of θ = 34% (red line) and 47% (green line). v = 50 m V s^{-1}, 0.5 M H_2SO_4, 25 °C. (For interpretation of the references to colour in this figure legend, the reader is referred to the web version of this article.)

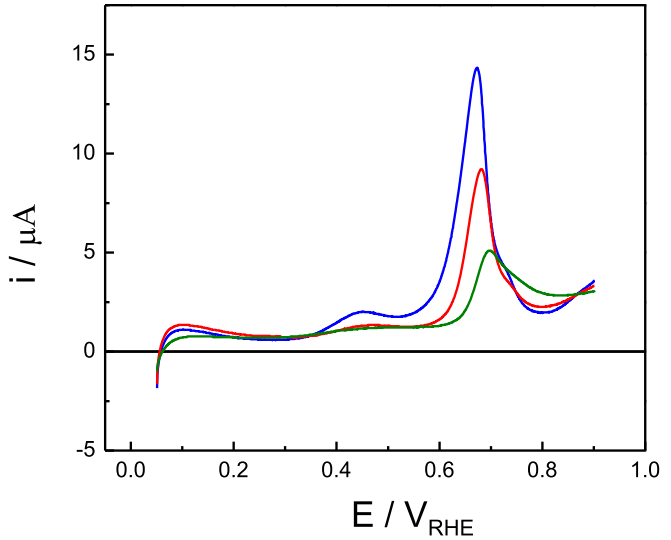

Fig. 2. CO stripping for Pt (blue line) and PtAu electrodes with Au coverage of θ = 34% (red line) and 47% (green line). E_{ad} = 0.070 V, v = 20 m V s^{-1}, 0.5 M H_2SO_4, 25 °C. (For interpretation of the references to colour in this figure legend, the reader is referred to the web version of this article.)

decreases, while that for the peak II increases at t_c higher than 10 s. Additionally, the position of peak I shifts towards more positive potentials at $t_c > 10$ s.

Thus, the profiles of the curves are similar at exposition times $t_c \leq 10$ s, in good agreement with the mechanism proposed for formic acid oxidation suggested by Capon and Parsons, in which a dual pathway is assumed [19]. The mechanism adopts an active reaction intermediate related to the current contribution at lower potentials (dehydrogenation path) [20], and a strong chemisorbed species, such as CO, which oxidizes at high overpotentials (dehydration path) [21,22]. It is remarkable that the current contribution associated with the oxidation of strongly adsorbed species becomes important at E > 0.6 V [18]. Stated briefly, the accepted mechanism for formic acid oxidation on Pt involves two well-defined pathways, i.e. direct (dehydrogenation) and indirect (dehydration) paths [18–20]. At Pt, the direct pathway is suppressed by strongly adsorbed CO on the metallic surface, which is rapidly generated by the HCOOH dehydration reaction at low overpotentials. Thus, the Pt surface is blocked by CO_{ad}, which is removed at high overpotentials

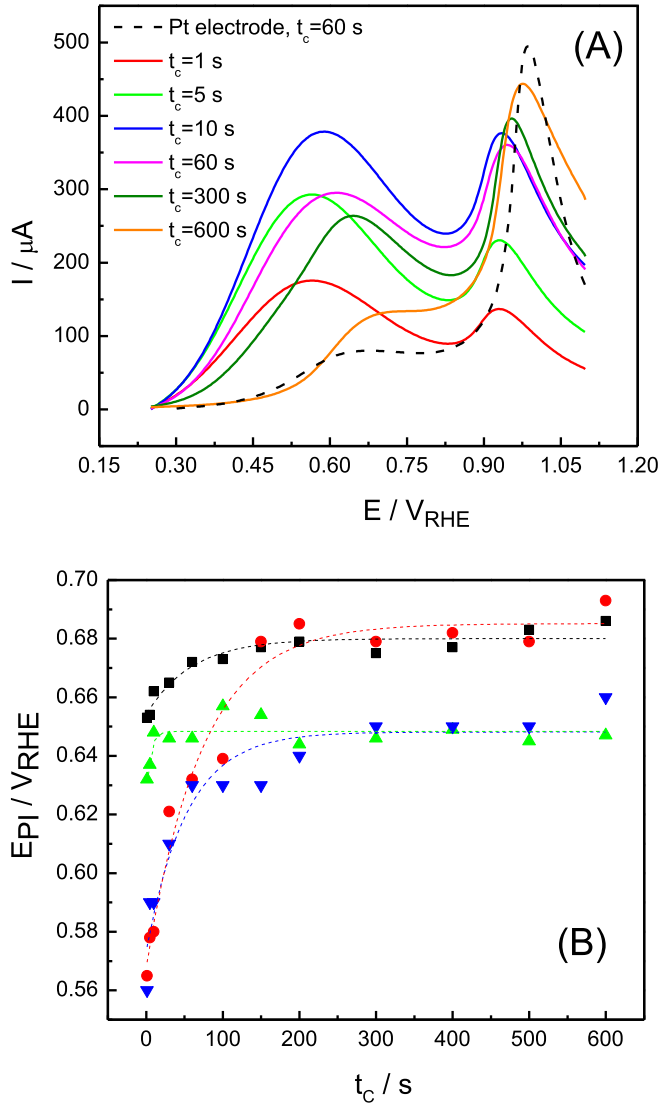

Fig. 3. (A) Linear sweep voltammetric curves as a function of the exposition time (t_c) at 0.25 V; Au coverage θ = 47%; 0.1 M HCOOH/0.5 M H_2SO_4; 50 m V s^{-1}; 25 °C. (B) $E_{p(I)}$ plotted as a function of the exposition time at 0.25 V. Pt electrode and 0.5 M $HClO_4$ (▲), Pt electrode 0.5 M H_2SO_4 (■); PtAu (θ = 47%) and 0.5 M $HClO_4$ (▼); PtAu (θ = 47%) and 0.5 M H_2SO_4 (●).

by adsorbed oxygenated species (OH_{ad}) that are produced by the water dissociation reaction.

Returning to the analysis of Fig. 3A, it is observed that at the highest exposition time investigated (600 s), the first contribution becomes to be a shoulder with a peak potential close to 0.72 V, and the anodic charge falls to a minimum. It is noticeable the shape of the LSV, which looks like the profile obtained with a Pt_{pc} electrode at t_c = 60 s (dashed line in Fig. 3A). The latter indicates the faster formation of strong chemisorbed species on Pt_{pc} than on Au-modified Pt_{pc} electrodes at 0.25 V, which inhibits the dehydrogenation pathway. In this context, the addition of gold atoms onto the Pt_{pc} electrode strongly modifies the behavior toward the formic acid oxidation reaction. The reaction rate of HCOOH dehydration (indirect pathway) is slower at gold-modified Pt electrodes than at Pt_{pc}, and consequently the direct pathway (dehydrogenation) is favored at the former. The last is reasonable, since the kinetic of the formic acid oxidation reaction strongly depends of the surface structure of the electrode [23–25].

Fig. 3B depicts the peak potential of the process happening at low overpotentials ($E_{p(I)}$) as function of tc for Pt_{pc} and PtAu electrodes in perchloric and sulphuric media. First of all, it is clear the effect of the anion on the peak potential, i.e. higher peak potentials are obtained for the experiments performed in sulphuric acid. In this sense, it is well known the strong adsorption of bi/sulfate species on Pt and Au, which compete with the formic acid for adsorption sites. Secondly, lower peak potentials are observed for gold-modified Pt_{pc} electrode in comparison with Pt_{pc} at both media and low tc. In this sense, the peak potential of the process (I) appears as an indirect evidence for the rate of CO formation (indirect pathway). Thirdly, high tc produces a decrease of the current density below 0.45 V with similar LSV profiles delivered for both materials. The latter is indicative of the direct pathway inhibition by strongly adsorbed species formation at high t_c.

T. Iwasita et al. studied the stripping of formic acid adsorbate formed on Pt(111) at 0.45 V between 50 and 360 s in sulphuric acid medium [26]. They found an increment of the anodic charge with the adsorption time, which was associated to the production of adsorbed CO from the acid dehydrogenation reaction. Surprisingly, the formic acid voltammogram recorded after 360 s of adsorption time resembles that of the present work achieved at PtAu electrode at t_c = 600 s. Reference [26] suggests slower formic acid adsorption on Pt(111) than Pt(110) and Pt(100) single crystal electrodes, though a better description may involve a slow formation of the indirect route at the close-packed surface. In fact, our results suggest that gold deposits mainly on Pt open structures and mostly Pt sites with (111) orientation remain free in the catalyst surface. Consequently, gold blocks active sites for the indirect pathway and acts as an apparent promoter for the direct route. This assumption is in agreement with a recent work of formic acid oxidation on gold adatoms decorated tetrahexahedral Pt nanocrystals, in which high catalytic currents with enhanced CO_2 production was observed at low overpotentials [27]. However, the CO oxidation reaction was not improved by the presence of the Au, and therefore it is suggested that the role of the Au is to promote the direct pathway.

Next study comprises the analysis of formic acid dehydration reaction. With this purpose formic acid was adsorbed at different potentials ($0.1 \leq E_{ad} \leq 0.6$ V) during 300 s, followed by electrolyte exchange at controlled potential, and after that the adsorbate stripping voltammogram was recorded. A typical stripping voltammogram is shown in Fig. 4A. In this kind of study, adsorbed CO is suggested to be the most important adsorbate specie produced in these conditions [28]. Fig. 4B shows the adsorbate (presumably CO) coverage obtained at different E_{ad} from formic acid adsorption on Pt and Au-modified Pt surfaces. Since gold does not adsorb CO in acidic medium, the adsorbate coverage was normalized to the Au-

free Pt surface. It is noticeable that CO coverage obtained from the formic acid dehydration reaction is significantly lower than that obtained from a complete adsorbed CO monolayer (Fig. 2). Additionally, it is important to note that adsorption of formic acid on gold-modified Pt_{pc} at 0.25 V for 300 s is an intermediate time to fulfill the complete formic acid dehydration reaction (Fig. 3), and therefore different adsorbed species than CO can survive on the surface. Furthermore, experiments depicted in Fig. 4 are quite different to those showed in Fig. 3, as different adsorption potentials were applied for each experiment, and therefore diverse amount of adsorbed species of different nature are expected. In this context, it is important to remind that the experiments depicted in Fig. 3 are carried out in solution containing formic acid, whereas the LSV shown in Fig. 4 are only associated to the oxidation of adsorbed species on the catalyst surface.

Fig. 4 shows an increment of the anodic charge with the gold coverage on Pt at $E_{ad} < 0.6$ V. If it is assumed that all the current charge is associated to CO_{ad} oxidation that was previously formed at controlled potential by formic acid dehydration, the results are in disagreement with those reported in the literature [18]. However, as was stated above, the anodic charge after 300 s may involve different adsorbed species than CO (at least) for gold modified Pt electrodes. In order to clarify these results FTIRS appears to be the most adequate technique.

In-situ FTIRS technique was extensively used to study the electrooxidation of formic acid on Pt and recently on gold-modified Pt catalysts [24,27]. Figs. 5 and 6 show the *in-situ* FTIR spectra obtained during the HCOOH oxidation on Pt and gold-modified Pt_{pc} (θ = 47%) materials, respectively. The following experimental strategy was adopted: i) introduction of the working electrode at fix potential of 0.6 V in the spectroelectrochemical cell containing formic acid solution and stabilization of the thin layer configuration (species are not adsorbed at this potential, see Fig. 4); ii) potential step from 0.6 to 0.05 V and acquisition of the reference spectrum; iii) steps of 0.05 V were applied in the positive direction up to 1.0 V, taking a spectrum at each potential (time for spectra acquisition: 40 s). In this way, the experiment starts with an electrode surface free of adsorbate species, and positive and negative bands represent the loss and gain of species at the sample potential, respectively.

Figs. 5 and 6 depict similar bands for both surfaces (Pt and gold-modified Pt), although they develop different potential dependence. At sample potentials higher than 0.5 V, four positive-going contributions are apparent at 1630, 1225, 1400 and 1720 cm^{-1}. The former is associated to the O–H bending mode of water, which disturb the spectral region between 1700 and 1400 cm^{-1}, while the others are associated to the consumption of formic acid [26]. Additionally, the negative band at 2343 cm^{-1} follows the CO_2 formation and the bipolar band at ca. 2070 cm^{-1} that shifts with the applied potential is attributed to linear adsorbed CO (CO_L) on Pt. The bipolar character of this band is mainly due to the Stark effect

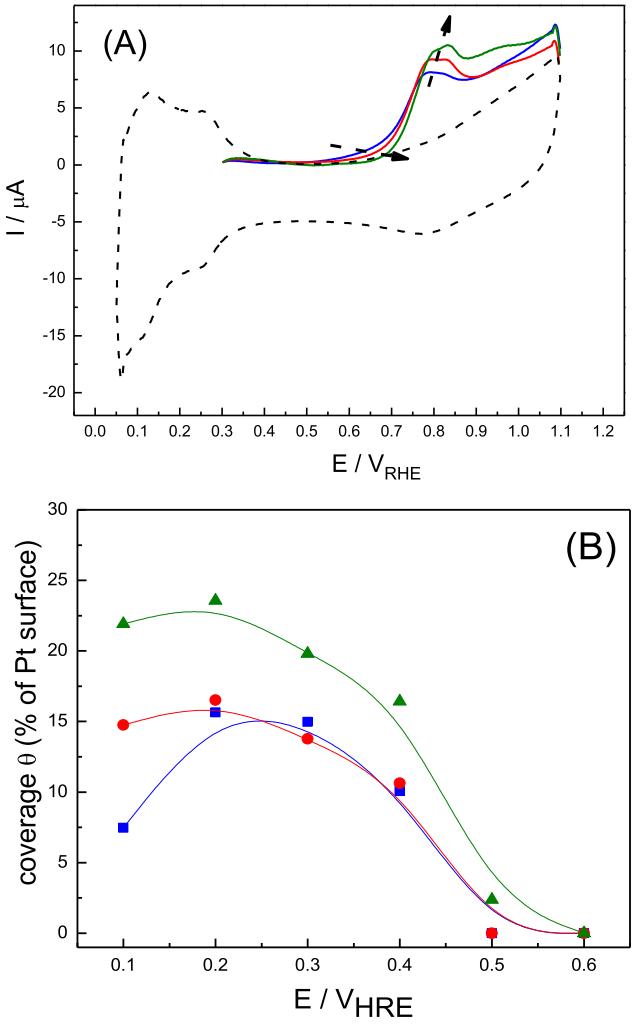

Fig. 4. (A) Anodic adsorbates stripping from HCOOH adsorption at 0.3 V for Pt (blue line), PtAu electrodes with Au coverage of θ = 34% (red line) and 47% (green line), and baseline cyclic voltammogram (second scan) showing the absence of HCOOH in the solution (dashed line). (B) Surface coverage as function of E_{ad} (V_{RHE}). Pt (■); PtAu θ = 34% (●); and PtAu θ = 47% (▲). 0.1 M HCOOH + 0.5 M H_2SO_4. 25 °C. (For interpretation of the references to colour in this figure legend, the reader is referred to the web version of this article.)

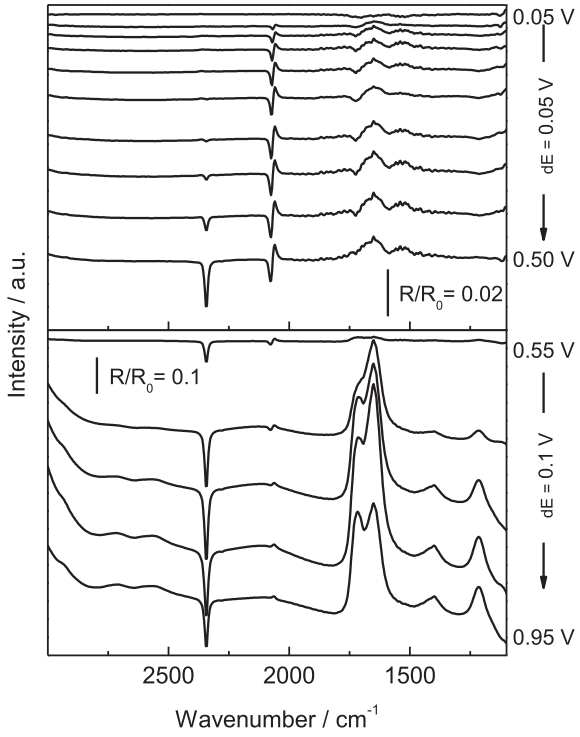

Fig. 5. In situ FTIR spectra for 0.5 M formic acid oxidation on Pt_{pc} in 0.5 M $HClO_4$. After 10 min at 0.6 V, the potential was stepped to 0.05 V. Then the potential was stepped positively from 0.05 up to 0.95 V. Reference potential: 0.05 V. The sample potentials are indicated at the right side of each panel.

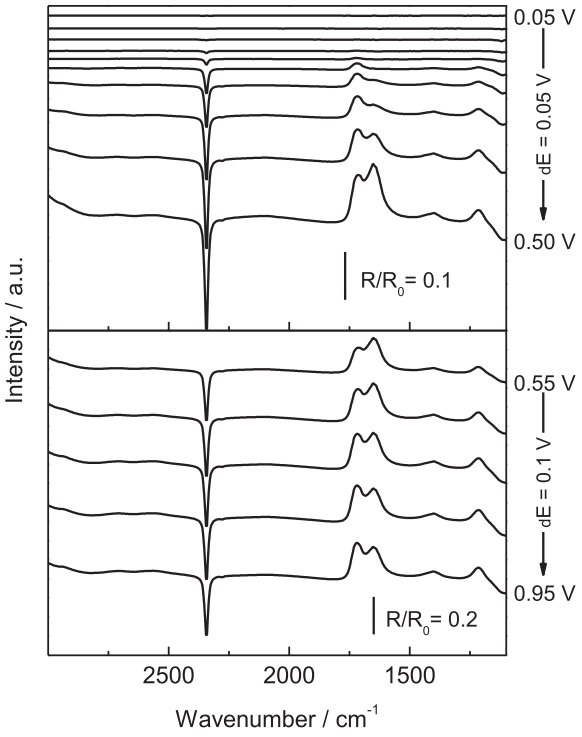

Fig. 6. In situ FTIR spectra for 0.5 M formic acid oxidation on PtAu ($\theta = 47\%$) in 0.5 M $HClO_4$. After 10 min at 0.6 V, the potential was stepped to 0.05 V. Then the potential was stepped positively from 0.05 up to 0.95 V. Reference potential: 0.05 V. The sample potentials are indicated at the right side of each panel.

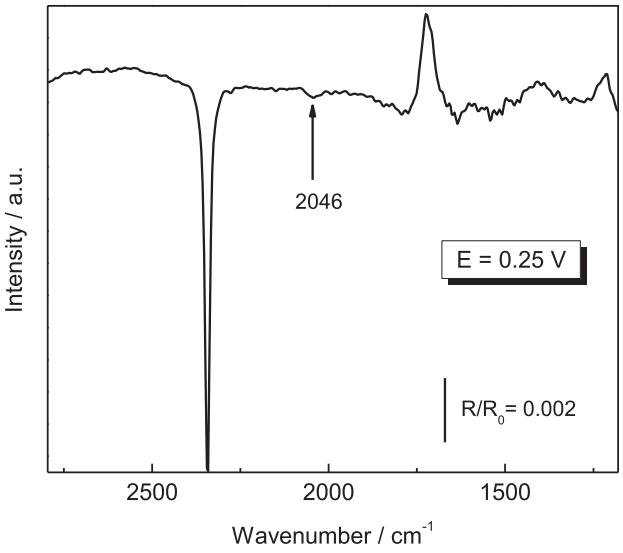

Fig. 7. Selected spectra from Fig. 6 corresponding to a sample potential of 0.25 V. The small production of CO_{ad} is shown.

(absorption frequency dependence with the applied potential) and indicates that this species is an adsorbate already present at the reference spectrum (R_0), i.e. at 0.05 V.

Main important findings are observed for the spectra recorded at E < 0.5 V, in which adsorbed carbon monoxide and soluble carbon dioxide are the main products at Pt_{pc} and gold-modified Pt_{pc} electrodes, respectively. Only small contribution of CO_{ad} appears as a negative band at 2043 cm^{-1} that shifts with the applied potential at higher values than 0.05 V at gold-modified Pt_{pc} (Fig. 7). Noticeable are the band intensities for CO_2 at 2343 cm^{-1}, which are higher for gold-modified Pt_{pc} than Pt_{pc} electrodes. All these results are in agreement with those exposed above and can be understood by inhibition of the dehydration route at gold modified Pt electrodes. Therefore, the main reaction happening at E < 0.5 V for Pt_{pc} is the dehydration (indirect pathway):

$$HCOOH + Pt \rightarrow H_2O + Pt{-}CO \quad (1)$$

At more positive potentials, CO_{ad} can be removed from the surface by adsorbed oxygenated species, which are previously formed from water dissociation reaction on Pt:

$$Pt + H_2O \rightarrow H^+ + e^- + Pt{-}OH \quad (2)$$

$$Pt{-}CO + Pt{-}OH \rightarrow CO_2 + 2\,Pt + H^+ + e^- \quad (3)$$

On the other hand, formic acid oxidation on gold-modified Pt_{pc} electrodes mainly follows the direct pathway (dehydrogenation route), in which adsorbed species may act as fast intermediate:

$$HCOOH + PtAu \rightarrow (\text{fast intermediate/s}) \rightarrow CO_2 + 2H^+ + 2e^- \quad (4)$$

From the results presented above, a more general picture of formic acid oxidation on Pt_{pc} and gold-modified Pt_{pc} electrodes in acidic media can be extracted. Reactions (1) and (2) are fast on Pt open structures, such as sites with (110) and (100) orientations, and defect sites (kink and step sites) [17,26]. Therefore, these sites are more tolerant to CO_{ad}, but also promote the indirect pathway, which produce the catalyst poison. On the other hand, Pt sites with (111) orientation are less reactive toward the water dissociation reaction (Eq. (2)) and therefore are easily poisoned by CO_{ad} [17]. However, the direct pathway of formic acid oxidation (Eq. (4)) is favored on Pt(111) single crystal electrodes, and therefore low production of the poisoning species is observed (Eq. (1)) [26].

An additional issue should be taken into account. The in-situ FTIR experiment shows the "stationary state" of surface at a given potential, once the equilibrium condition of the each species involved in the mechanism has been attained. In fact, under this condition, the method is unable to determinate the chemical nature of such fast intermediate, and its identity is merely speculative. On the other hand, the FTIRS demonstrates that the CO coverage at the equilibrium (balance between CO formation and the subsequent CO elimination) is extremely low. However, the absence of CO bands in the IR spectra is not enough to discard its participation on the mechanism proposed.

In the present paper, Au is spontaneously deposited on Pt surface, while the traditional "wet" method implies a first step of Cu under potential deposition (UPD) onto Pt substrate and the subsequent galvanic exchange of Cu by Au [3–5]. Using the spontaneous deposition method is observed that gold mainly deposits on Pt sites with (110) and (100) orientations and on Pt low-coordinated sites, and therefore mostly Pt sites with (111) orientation are exposed (remains free) at the surface. The consequence of gold deposition on Pt_{pc} is clearly observed in the exposed results, in which the dehydrogenation route predominates during the formic acid oxidation reaction. Gold may also enhance the activity toward CO and formic acid oxidation reactions at higher potential than 0.5 V [29] although a promoter effect by gold toward both reactions cannot be discarded at low overpotentials. Consequently, the behavior of gold deposition on Pt at lower potential than 0.5 V is more like a third body effect. Thus, the indirect pathway is slower (blocked) at gold-modified Pt electrodes and the direct route appears as the predominant. These are the main reasons for the high activity developed by the gold-modified electrode toward the

formic acid oxidation at lower potential than 0.5 V. In order to discard the effect by chloride ions, during the Pt surface modification, additional electrochemical experiments were performed (see Supplementary Information). These results indicate the absence of chloride species in the synthesized gold-modified Pt_{pc} electrodes.

The great similitude of results achieved with gold-modified Pt_{pc} electrodes and those reported by T. Iwasita et al. for formic acid oxidation onto Pt(111) electrode seems reasonable. In this sense, a similar mechanism for formic acid oxidation reaction may occur at gold-modified Pt_{pc} (described in the present work) and Pt(111) surfaces. In fact, it was observed in Fig. 1 that Au deposition effectively affects the hydrogen adsorption on Pt(110) and Pt(100) sites, indicating a preferential Au deposition on these sites. In this context, it is well-known that open surfaces such as (110), (100) and defect sites are more reactive to formic acid oxidation reaction than compact surfaces (e.g. Pt(111)), as revealed by studies using Pt single crystals electrodes [25]. The same study confirms that Pt(100) and Pt(110) structures are the most prone to be poisoned by adsorbed CO resulting from the HCOOH dehydration reaction, while the adsorption of HCOOH to produce adsorbed CO on Pt(111) single crystal is a relatively slow process [25]. All these results are in good agreement with the observed behavior for the gold-modified Pt_{pc} electrode described and analyzed in the present manuscript.

On the other hand, the CO stripping experiments (Fig. 2) also support the idea of a selective Pt surface modification by Au atoms, in which a lower tolerance to CO is observed with the rise of Au coverage. The latter indicates suppression of Pt active sites (open Pt surface sites) for water dissociation (adsorbed oxygenated species formation, i.e. OH_{ad}) which are crucial to oxidize adsorbed CO [17]. In this sense, it is reported that the activity towards water dissociation depends on the surface structure and platinum with (111) orientation is the less reactive surface in acidic media [17]. Based on this set of observations, we tentatively ascribe our results to a selective modification of the Pt surface, in which maintains unmodified the Pt (111) contribution. Regardless of previous stated, the gold attached to the surface may also acts as a physical barrier for the surface mobility of the adsorbed molecules, and this contribution can not be discarded [16].

Then, the high activity towards HCOOH electrooxidation exhibited by gold-modified Pt_{pc} electrodes at $E < 0.5$ V (Fig. 3A) can be explained in terms of two competitive effects: i) the slow CO poisoning rate due to the Au blocking of reactive Pt open ((110) and (100)) sites; and ii) the relatively high scan rate that allows, in short times, to reach potentials in which the scarcely adsorbed CO can be easily removed from the surface. For example, during a typical voltammetric in the positive going scan, with an initial potential of 0.05 V and a scan rate between 0.020 and 0.1 V s^{-1}, the electrode potential reaches 0.6 V in less than 30 s. In contrast, the direct pathway (dehydrogenation) inhibition by HCOOH adsorption and subsequent dehydration to produce adsorbed CO take at least 300 s at fix potential of 0.25 V (Fig. 3B).

Finally, our results suggest that the faradaic current contribution during the formic acid oxidation on gold-modified Pt_{pc} electrodes at low overpotentials is mainly associated to the direct pathway due to the CO formation reaction (indirect pathway) is inhibited.

4. Conclusion

The formic acid electrooxidation on Pt_{pc} and Pt_{pc} modified by spontaneous deposition of Au was studied by FTIRS and conventional electrochemical techniques. Two main operative routes were founded during the formic acid oxidation reaction, i.e. dehydration (indirect route) and dehydrogenation (direct route) pathways. These routes mainly depend on the applied potential and the surface structure.

The surface structure becomes of paramount importance at low overpotentials ($E < 0.5$ V). At low overpotentials, the high faradaic current contribution developed by the Au-modified Pt_{pc} electrodes is associated with a slow CO poisoning rate, which is produced by Au deposition on Pt active sites for formic acid dehydration reaction. Consequently, the indirect pathway is inhibited and the direct pathway becomes the main route during the formic acid oxidation on Au-modified Pt_{pc} materials. On the other hand, formic acid dehydration occurs at potentials as low as 0.05 V at Pt_{pc} electrode. The high density of surface sites with (110) and (100) orientation appears as the main responsible for the fast dehydration reaction and consequently the indirect route is the operative at Pt_{pc} electrode.

Finally, the high activity towards HCOOH observed by the CV experiments can be explained in terms of two competitive effects: i) the slow CO poisoning rate due to the Au blocking of reactive Pt open ((110) and (100)) sites; and ii) the relatively high scan rate that allows, in short times, to reaching potentials in which the scarcely adsorbed CO can be easily removed from the surface.

Acknowledgments

The authors gratefully acknowledge financial support given by the Spanish MINECO under the project CTQ2011-28913-C02-02 and PRI-AIRBAR-2011-1307 for the cooperation between both groups, and ANPCyT (Argentine, project PICT-2010-2421) for the financial support. P.S.C acknowledges CONICET (Argentine) for the doctoral fellowship. J.F-M. is indebted to the ACIICI (Gobierno de Canarias) for the predoctoral fellowship. C.A. Barbero and G.A. Planes are permanent research fellows of CONICET.

Appendix A. Supplementary data

Supplementary data related to this article can be found at http://dx.doi.org/10.1016/j.jpowsour.2015.07.005.

References

[1] K.-J. Jeong, C.M. Miesse, J.-H. Choi, J. Lee, J. Han, S.P. Yoon, S.W. Nam, T.-H. Lim, T.G. Lee, J. Power Sources 168 (2007) 119–125.
[2] X. Ji, K.T. Lee, R. Holden, L. Zhang, J. Zhang, G.A. Botton, M. Couillard, L.F. Nazar, Nat. Chem. 2 (2010) 286–293.
[3] R. Wang, C. Wang, W.-B. Cai, Y. Ding, Adv. Mater. 22 (2010) 1845–1848.
[4] X. Bi, R. Wang, Y. Ding, Electrochim. Acta 56 (2011) 10039–10043.
[5] S. Zhang, Y. Shao, G. Yin, Y. Lin, J. Power Sources 195 (2010) 1103–1106.
[6] S. Wang, X. Wang, S.P. Jiang, Phys. Chem. Chem. Phys. 13 (2011) 6883–6891.
[7] J. Joo, T. Uchida, A. Cuesta, M.T.M. Koper, M.J. Osawa, Am. Chem. Soc. 135 (27) (2013) 9991–9994.
[8] M. Neurock, M. Janik, A. Wieckowski, Faraday Discuss. 140 (2008) 363–378.
[9] A. Cuesta, ChemPhysChem 12 (2011) 2375–2385.
[10] M. Ojeda, E. Iglesia, Angew. Chem. Int. Ed. 48 (2009) 4800–4803.
[11] R. Muralidharan, M. McIntosh, X. Li, Phys. Chem. Chem. Phys. 15 (2013) 9716–9725.
[12] K. Arihara, F. Kitamura, T. Osaka, K. Tokuda, J. Electroanal. Chem. 510 (2001) 128–135.
[13] J. Solla-Gullón, P. Rodriguez, E. Herrero, A. Aldaz, J.M. Feliu, Phys. Chem. Chem. Phys. 10 (2008) 1359–1373.
[14] V. Stamenkovic, M. Arenz, B.B. Blizanac, K.J.J. Mayrhofer, P.N. Ross, N.M. Markovic, Surf. Sci. 576 (2005) 5145–5157.
[15] J. Clavilier, K. Elachi, A. Rodes, Chem. Phys. 141 (1990) 1–14.
[16] F. Maillard, M. Eikerling, O.V. Cherstiouk, S. Schreier, E. Savinova, U. Stimming, Faraday Discuss. 125 (2004) 357–377.
[17] G. García, M.T.M. Koper, ChemPhysChem. 12–11 (2011) 2064–2072.
[18] H.-X. Liu, N. Tian, M.P. Brandon, J. Pei, Z.-C. Huangfu, C. Zhan, Z.-Y. Zhou, C. Hardacre, W.-F. Lin, S.-G. Sun, Phys. Chem. Chem. Phys. 14 (2012) 16415–16423.
[19] A. Capon, R. Parsons, J. Electroanal. Chem. 44 (1973) 239–254.
[20] V. Grozovski, F.J. Vidal-Iglesias, E. Herrero, J.M. Feliu, ChemPhysChem 12 (2011) 1641–1644.
[21] B. Beden, A. Bewick, C. Lamy, J. Electroanal. Chem. 150 (1983) 505–511.
[22] M. Arenz, V. Stamenkovic, T.J. Schmidt, K. Wandelt, P.N. Ross, N.M. Markovic, Phys. Chem. Chem. Phys. 5 (2003) 4242–4251.
[23] V. Grozovski, V. Climent, E. Herrero, J.M. Feliu, J. Phys. Chem. C 114 (2010)

13802–13812.
[24] V. Grozovski, V. Climent, E. Herrero, J.M. Feliu, ChemPhysChem 10 (2009) 1922–1926.
[25] V. Grozovski, V. Climent, E. Herrero, J.M. Feliu, Phys. Chem. Chem. Phys. 12 (2010) 8822–8831.
[26] T. Iwasita, X. Xia, E. Herrero, H.-D. Liess, Langmuir 12 (1996) 4260–4265.
[27] H.-X. Liu, N. Tian, M.P. Brandon, J. Pei, Z.-C. Huangfu, C. Zhan, Z.-Y. Zhou, C. Hardacre, W.-F. Lin, S.-G. Sun, Phys. Chem. Chem. Phys. 14 (2012) 16415–16423.
[28] Y.-X. Chen, M. Heinen, Z. Jusys, R.J. Behm, Langmuir 22 (2006) 10399–10408.
[29] G.L. Beltramo, T.E. Shubinaand, M.T.M. Koper, ChemPhysChem. 6 (2005) 2597–2606.